Finite-Element Thermal-Structural Analyses of a Cable-Stiffened Orbiting Antenna

Earl A. Thornton* and Pramote Dechaumphai†
Old Dominion University, Norfolk, Virginia
and
Ajay K. Pandey‡
Virginia Polytechnic Institute and State University, Blacksburg, Virginia

Finite-element thermal-structural analyses of a cable-stiffened orbiting antenna are presented. The determination of prestresses in the antenna is described first. Heating and thermal analyses for orbiting space structures are then discussed briefly. Structural deformations and stresses are presented for three finite-element structural analysis approaches: 1) small deflections, 2) stress-stiffening, and 3) large deflections. The accuracy of the three analysis approaches is evaluated for the orbiting antenna at different prestress levels.

Nomenclature

a_e = surface emissivity
a_s = surface absorbtivity
A_q = incident heating area
A_r = surface radiation area
$[B]$ = matrix containing direction cosines of structural numbers
c = specific heat
E = modulus of elasticity
F_x,F_y,F_z = member force components in Cartesian coordinates
$\{F\}$ = member force vector
$\{F\}_{\epsilon_0}$ = finite-element force vector due to thermal strain
$\{F\}_{\sigma_0}$ = finite-element force vector due to prestress
$[K]$ = finite-element stiffness matrix
L = finite-element length
q = total incident heating rate
q_a = Earth-reflected solar heating rate
q_e = Earth-emitted heating rate
q_s = solar heating rate
t = time
T = element temperature
u = displacement in local x coordinate
$u_1,u_2;v_1,v_2;w_1,w_2$ = nodal displacements in local, x, y, and z coordinates, respectively
x,y,z = Cartesian coordinates
α = orbital position, deg
ϵ = total strain
ϵ_0 = thermal strain
ρ = density
σ = element stress
σ_0 = element prestress

Presented as Paper 85-0693 at the AIAA/ASME/ASCE/AHS 26th Structures, Structural Dynamics and Materials Conference, Orlando, FL, April 15-17, 1985; received Aug. 12, 1985; revision received Feb. 17, 1986.

*Professor, Mechanical Engineering and Mechanics Department. Member AIAA.

†Research Associate, Mechanical Engineering and Mechanics Department. Member AIAA.

‡Graduate Research Assistant; formerly Graduate Research Assistant, Old Dominion University, Norfolk, VA.

Introduction

PAST and proposed Space Shuttle flights have brought the world into the era of space transportation. In the near future, large space structures will be placed in Earth orbits. Two basic classes of orbiting large space structures proposed for communications, Earth observation, and remote sensing are large antennas and space platforms. To assure satisfactory performance of the orbiting structures, detailed analyses of structural integrity and stability are required. These analyses include prediction of structural deformations introduced by cyclic heating on the structure during the orbit. Deformations must be kept within design-allowable tolerances to assure satisfactory structural performance. Due to the large size of these structures ground testing is not possible, and thus reliable analyses are required to predict structural deformations accurately.

To increase the structural stability and to provide additional stiffness to the structural system, the concept of prestressed cables and membranes has been proposed for some designs.[1-3] Prestressed structures, such as the hoop-column antenna, shown in Fig. 1, can provide ease of deployment while maintaining low mass and stability. Cable-stiffened space structures are difficult to analyze because: 1) members have prestresses, 2) cables cannot take compressive forces, and 3) large deformations may be experienced. Accurate prediction of structural deformations depends primarily on the heating, thermal, and structural analyses techniques adopted. The present work uses an integrated finite element approach for prediction of thermally induced structural deformations of a cable-stiffened orbiting antenna. The purpose of this paper is to investigate the accuracy of three finite-element structural analysis approaches as a function of the magnitudes of the prestresses for the thermal environment of a typical antenna orbit. The three approaches are: 1) small-deflection, 2) stress-stiffening, and 3) large-deflection structural analyses.

In the balance of this paper the analyses of the orbiting structural prestresses and the environmental heating are first highlighted. Then the basic equations for finite-element thermal-structural analyses are summarized. A cable-stiffened orbiting hoop-column antenna is described next, and typical structural deformations results are presented. Finally, the results obtained from the three finite-element structural analysis approaches are evaluated and discussed for different prestress levels.

Integrated Finite-Element Analysis

To predict the thermally induced structural deformations of cable-stiffened structures, a series of analyses must be per-

formed. These include: 1) a prestress analysis, 2) a heating rate analysis, 3) a thermal analysis, and 4) a structural analysis. The complete analysis procedure is shown in Fig. 2.

Prestress Analysis

Many proposed large space structures use prestressed cables and rods to provide stiffness and stability to the structural system. Before performing a structural analysis, a prestress analysis is required to determine the tensile or compressive forces and stresses in each member. The basic requirements for the prestress analysis are that the structures: 1) maintain the required geometry, and 2) be in static equilibrium.

To determine the member forces and stresses, a truss-type structure is assumed to be statically determinant. The equilibrium equations at each joint are written as follows:

$$\Sigma F_x = 0 \tag{1a}$$

$$\Sigma F_y = 0 \tag{1b}$$

$$\Sigma F_z = 0 \tag{1c}$$

where F_x, F_y, and F_z are the member force components in Cartesian coordinates. For a truss-type structure with n joints and m members, there are $3n$ equilibrium equations and m unknown member forces. The preceding equilibrium equations for the entire structure can then be written in matrix form as

$$\underset{(3n^*m)}{[B]} \quad \underset{(m^*1)}{\{F\}} = \underset{(3n^*1)}{0} \tag{2}$$

where $[B]$ contains direction cosines of the members, and $\{F\}$ is an unknown vector of the member forces.

Since some of the member forces are specified, the corresponding columns in the $[B]$ matrix are multiplied by the specified forces and transferred to the right-hand side of the equation. Depending on the total number of equations and total number of unknown member forces, either additional forces are specified or extra equations are discarded to provide the number of equations equal to the number of unknowns. Thus, the unknown member forces can be determined by solving the final linear simultaneous equations.

Heating Analysis

During orbit, structural deformations and thermal stresses are produced due to environmental heating. To perform the structural analysis, the structural temperature distribution is needed to compute the thermally equivalent nodal forces. The structural temperature distribution can be computed if the environmental heating is known.

The environmental heat sources applied to the space structure are solar heating, Earth-emitted heating, and Earth-reflected solar heating. Earth-emitted heating and Earth-reflected solar heating depend on altitude and orientation of the structure. The total incident heating rate q (per unit area) on the structure is given by

$$q = q_s + q_e + q_a \tag{3}$$

where q_s, q_e, and q_a are the incident solar heating, incident Earth-emitted heating, and Earth-reflected solar heating rates, respectively.

If the structure enters the Earth's shadow during the orbit, the heating on the structure is greatly reduced due to the absence of solar heating. The duration of the shadowing depends upon the altitude of the orbit. The present study uses a geosynchronous orbit, which has an altitude of 42,000 km. The heating on a member depends strongly on a member's orientation with respect to the solar vector and, consequently, may vary significantly from member to member and with time during the orbit.

Thermal Analysis

Once the heating rate on the structural member has been determined, the structural temperature distribution at different orbital positions can be computed. Basic types of heat transfer for a typical space structural element are member conduction and surface radiation. For a structure made from composite materials such as graphite epoxy, member heat conduction is small due to the low material thermal conductivity. Thus, for composite materials, the temperature is nearly uniform along the member length. For simplicity, temperature gradients through the thickness of a member are disregarded. This latter assumption is a very good approximation for the thin cables of graphite epoxy considered in this study. With these assumptions, the governing differential equation for a structural member is

$$\rho c V \frac{\partial T}{\partial t} + \sigma a_e A_r T^4 = a_s A_q q(t) \tag{4}$$

where ρ is the density, c the specific heat, V the member volume, σ the Stefan-Boltzmann constant, a_e the surface emissivity, A_r the element radiation area, a_s the surface absorbtivity, A_q the incident heating area, and $q(t)$ the incident rate per unit area.

The above differential equation, Eq. (4), is used to formulate an isothermal finite-element via the method of weighted residuals.[4] Using this concept, temperatures for each member can be computed independently. A typical equation is solved using the Crank-Nicolson finite-difference technique for transient time marching and Newton-Raphson iteration at each time step. The temperature distribution of the structure may be determined at each time step for the entire orbit in this manner.

Structural Analysis

To derive the structural finite-element equations for a one-dimensional rod or cable element, the principle of minimum potential energy is employed. The stress-strain relation for a member with prestress σ_0 and thermal strain ϵ_0 is given by

$$\sigma = E(\epsilon - \epsilon_0) + \sigma_0 \tag{5}$$

where σ is the element stress, E the modulus of elasticity, and ϵ the total strain. Three structural analysis approaches are investigated: 1) a small-deflection analysis, 2) a stress-stiffening analysis, and 3) a large-deflection analysis.

For small-deflection analysis, the strain-displacement relation is

$$\epsilon = \frac{\partial u}{\partial x} = \frac{u_2 - u_1}{L} \tag{6}$$

where u_1 and u_2 are the element nodal displacements in the local x coordinate, and L is the element length. The finite-element equations for a quasistatic analysis, where the structural inertia effect is neglected, have the form

$$[K]\{u\} = \{F\}_{\epsilon_0} + \{F\}_{\sigma_0} \tag{7}$$

where $[K]$ is the element stiffness matrix, and $\{u\}$ is the vector of unknown nodal displacements. The right-hand side of Eq. (7) contains the equivalent nodal forces associated with the element thermal strain and prestress, respectively.

For the stress-stiffening and large-deflection analyses, small axial strain is assumed and the strain-displacement relation is

$$\epsilon = \frac{u_2 - u_1}{L} + \frac{1}{2}\left(\frac{v_2 - v_1}{L}\right)^2 + \frac{1}{2}\left(\frac{w_2 - w_1}{L}\right)^2 \tag{8}$$

where v_1, v_2 and w_1, w_2 are the nodal displacements in the local y and z coordinates, respectively. The finite-element

equations are nonlinear in the form

$$[K(u)]\{u\} = \{F\}_{\varepsilon_0} + \{F\}_{\sigma_0} \tag{9}$$

where $[K(u)]$ is the stiffness matrix that depends on the unknown nodal displacement. To solve these nonlinear equations an iterative technique is required.

The stress-stiffening analysis uses two iterations. For the first iteration, all nodal displacement components which appear in the element stiffness matrix are zero. Nodal displacement components computed in the first iteration are then used as the approximate solution for the second iteration, which gives the stress-stiffening results.

In the large-deflection analysis,[5] the Newton-Raphson iteration method is used. The iteration process is terminated when the ratios of nodal displacement increments to their displacements are less than a specified tolerance (10^{-2} was used in this study).

Further details of the analyses appear in Ref. 6.

Analysis of Hoop-Column Antenna

A top view of the finite-element model of the hoop-column antenna is shown in Fig. 3. The finite-element model consists of 123 nodes and 387 elements. The hoop and column are represented by rod elements, and cables are represented by cable elements. In addition, 192 fictitious cable elements were added for structural stability. The fictitious cable elements have a very low modulus of elasticity compared to the other elements of the structure and have a zero coefficient of thermal expansion. Further details of the model, such as the member cross-sectional areas and material properties, appear in Ref. 6.

Structural Prestresses and Temperatures

The structure's geometric symmetry is used in the prestress analysis; a typical section is shown in Fig. 4. Six member forces (element numbers 5, 10, 15, 16, 17, 18) are specified, and the prestress program is used to compute other member forces and stresses. The computed stresses are used as the member prestresses in the structural analysis. The fictitious elements have no prestresses.

In the determination of member temperatures, the structure is assumed to be in a geosynchronous orbit oriented as shown in Fig. 5 with the antenna surface pointing toward Earth. The member incident heating is maximum when the member is perpendicular to the solar heating vector. Member heating drops when the member is either parallel to the solar vector or in the Earth's shadow. Member heating rates are used to compute member temperatures in the thermal analysis. The heating and thermal analyses are performed at different orbital positions up to an orbital angle of 200 deg. A temperature variation from 310 to 90 K is observed for a typical member during passage through the Earth's shadow.

Structual Deformations

Using the prestresses and temperatures obtained, the small-deflection, stress-stiffening, and large-deflection structural analyses are performed to compute nodal deflections and member stresses at different orbital positions. The three analyses predict similar distributions of nodal displacements and member stresses. The hoop and antenna of the structure are in compression at all times during the orbit. Buckling of these members has not been considered.

Figures 6–9 present deflection results predicted using the large-deflection theory approach. Figure 6 shows the Z-displacement histories for two typical nodes on the antenna's surface. During orbit, points on the antenna's surface move toward and away from the Earth, i.e., $\pm Z$ displacements take place. The maximum Z displacement of 20 mm occurs at a node on the antenna's surface nearest to the hoop when the antenna passes through the Earth's shadow. A significant displacement of 15 mm occurs at the same node at an orbital position of 90 deg. The Z displacements of the antenna surface at three orbital positions are shown in Fig. 7. Figure 8 shows the Z displacements of four panels at the 90-deg orbital position. Figure 9 shows displacement contours on the antenna's surface. The figures show that antenna surfaces near the hoop have maximum deflection and the displacements are nonaxisymmetric. Displacements in the central region of the antenna's surface are relatively small. The stress variation for a typical element is ±8% from a prestress value of 60 MPa. Thus, thermally induced member forces are relatively small compared to pretension forces.

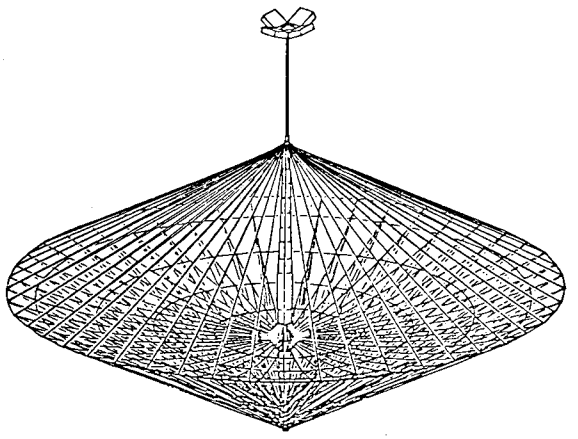

Fig. 1 Cable-stiffened hoop-column antenna.[1]

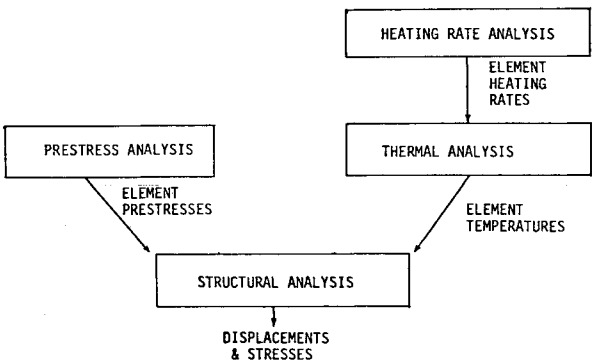

Fig. 2 Thermal-structural analysis procedure.

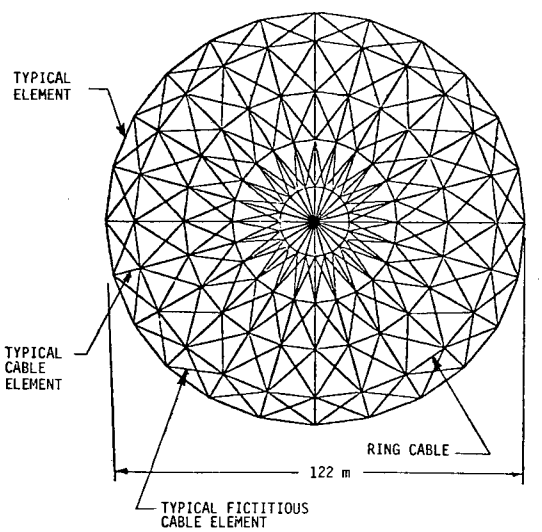

Fig. 3 Top view of the finite-element model of the hoop-column antenna.

ELEMENT NO.	FORCE (N)	PRESTRESS (MPa)
1	121.7	16.2
2	134.1	17.8
3	154.2	20.5
4	189.1	25.2
5	452.0	60.2
6	37.1	32.0
7	22.2	19.1
8	33.2	28.6
9	26.2	226.5
10	140.0	30.2
11	407.5	14.8
12	-5968.4	-25.1
13	-6681.1	-28.1
14	-3291.3	-12.3
15	25.0	84.0
16	20.0	67.2
17	15.0	50.4
18	10.0	33.6

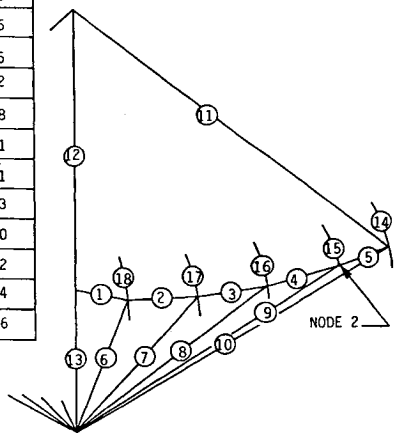

Fig. 4 Member prestresses for hoop-column antenna.

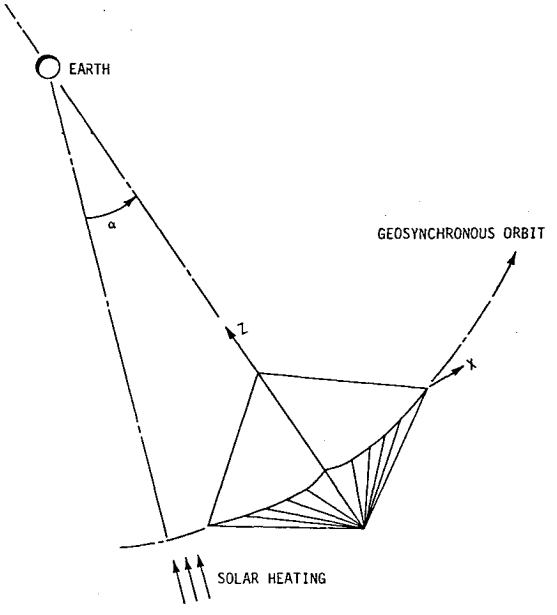

Fig. 5 Orientation of hoop-column antenna in Earth orbit.

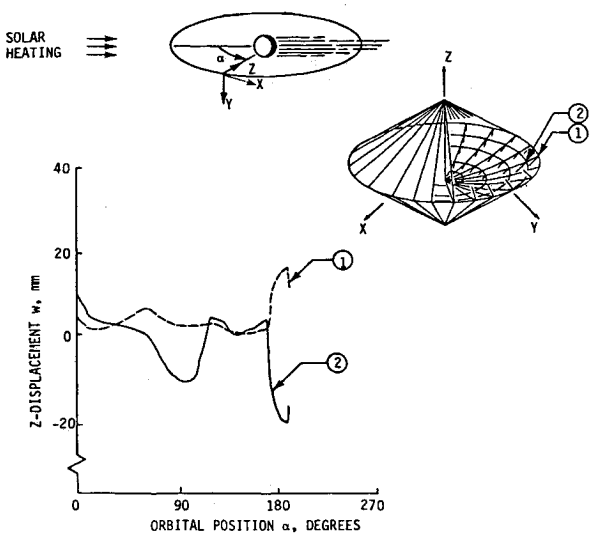

Fig. 6 Displacement histories for two typical nodes on the hoop-column antenna.

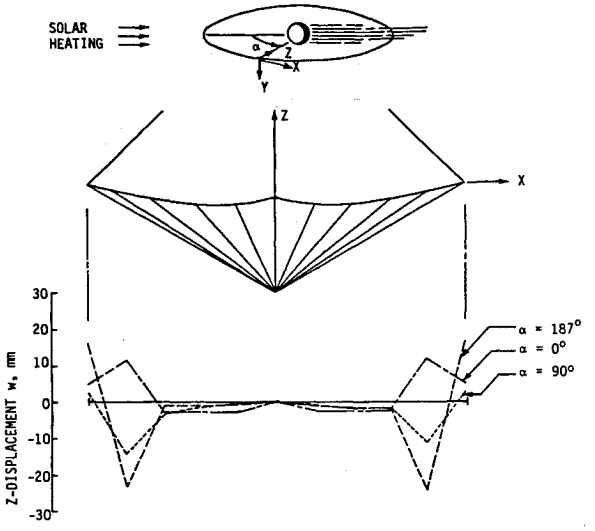

Fig. 7 Displacement distributions at different orbital positions for hoop-column antenna.

Comparative Structural Analyses Accuracy

To evaluate the structural analyses' accuracy, the small-deflection, stress-stiffening, and large-deflection analyses are performed at three typical prestress levels. Member 5 (see Fig. 4) has a force of 226 N for prestress level 1, 452 N for prestress level 2, and 4520 N for prestress level 3. The third prestress level is a hypothetical prestress level assumed for evaluation of the three structural analysis techniques. At this prestress some of the members may exceed design-allowable stresses in tension or compression. Displacements of node 2, Fig. 4, at these prestress levels for the three structural analysis techniques are given in Table 1 at the 0, 90, and 187-deg orbital positions.

For all three prestress levels, the small-deflection analysis overestimates displacements compared to the stress-stiffening and large-deflection analyses. With increasing prestress, the small-deflection analysis results remain almost unchanged, but the stress-stiffening and large-deflection results decrease significantly, predicting relatively small deflections at higher prestress.

At NASA design prestresses (level 2), results from the three analysis techniques differ significantly. The small-deflection analysis predicts 11, 21, and 23% more deflection than the large-deflection analysis at the three orbital positions. The stress-stiffening analysis predicts 5, 0.5, and 0.1% more deflection than the large-deflection analysis at these positions. These results show that at NASA design prestresses, a stress-stiffening analysis can be used to predict deflections with acceptable accuracy.

Comparison of CPU times gives a ratio of 1:11:16 for the analyses. Although the small-deflection analyses is efficient in computer time, the results of this analysis may not have acceptable accuracy. A stress-stiffening analysis can give, depending on the prestress, results of acceptable accuracy. Considering these facts, the use of the stress-stiffening method can be recommended for structural analysis of the hoop-column antenna at NASA design prestresses. The large-

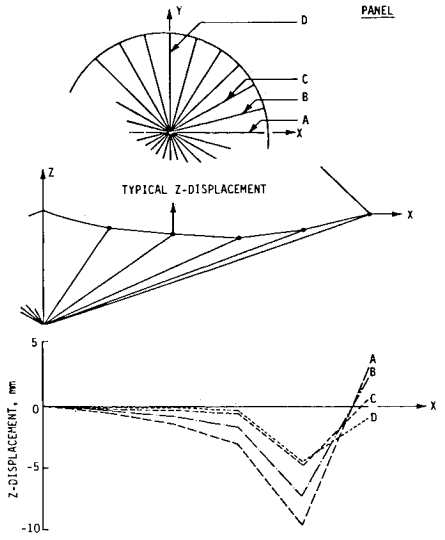

Fig. 8 Displacement of typical panels on antenna surface for hoop column at 90-deg orbital position.

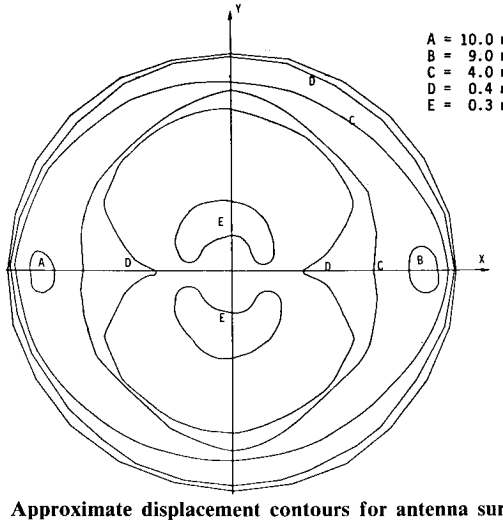

Fig. 9 Approximate displacement contours for antenna surface at 90-deg orbital position.

Table 1 *Z*-deflection comparison for node 2 (Fig. 4) for different orbital positions and prestress levels

Type of analysis	Orbital position, deg		
	0	90	187
Prestress level 1 ($F_5^* = 226$ N)[a]			
Linear	11.62[b]	−11.40	−24.03
Stress stiffening	11.31	−10.40	−21.68
Nonlinear	10.98	−10.37	−21.66
Prestress level 2 ($F_5 = 452$ N)			
Linear	11.62	−11.40	−24.03
Stress stiffening	11.01	−9.49	−19.60
Nonlinear	10.45	−9.44	−19.58
Prestress level 3 ($F_5 = 4520$ N)			
Linear	11.65	−11.37	−24.00
Stress stiffening	7.89	−2.15	−2.97
Nonlinear	6.39	−2.25	−2.90

[a] F_5 is the pretension in member 5 (see Fig. 4). [b] All z displacements are expressed in mm.

deflection analysis method is recommended as a more general and more expensive technique for all prestress levels.

Concluding Remarks

Finite-element thermal-structural analyses of a cable-stiffened orbiting antenna are presented. The determination of cable prestresses is first described. Heating and thermal analyses are then discussed. Analyses of structural deformations and stresses are performed using small-deflection, stress-stiffening, and large-deflection techniques.

To analyze the cable-stiffened orbiting antenna, a prestress analysis is first performed to determine the structural prestresses. The structural incident heating history is then computed, and the thermal analysis is performed to compute the structural temperature distribution. The structural prestresses and temperature distribution are used in the structural analysis for computation of deformations and stresses.

Thermal-structural analyses of the prestressed hoop-column antenna showed that the variation of member stress due to thermal effects during the orbit is small compared to the prestress. The effect of member prestress levels on the accuracy of the analysis techniques is evaluted using comparisons of structural deformations. At low prestresses, the three analyses predict similar deformations. With increasing prestress, deformations obtained from the small-deflection analysis remain almost unchanged, whereas a large decrease in deformations is predicted by the stress-stiffening and large-deflection analyses. Although the small-deflection analysis is efficient in computer time, the results may not have acceptable accuracy. A stress-stiffening analysis is not as expensive as a large-deflection analysis and can provide, depending on the prestress, results of acceptable accuracy. The stress-stiffening method can be recommended for structural analysis of the hoop-column antenna at NASA design prestresses.

The large-deflection analysis technique is recommended as a general and more expensive technique for all prestress levels. The results have shown that accuracy in predicting the deformation and stress for cable-stiffened structures strongly depends on the prestress. The large-deflection analysis technique produced accurate results over a wide prestress range and is recommended as a general analysis approach for thermal-structural analysis of cable-stiffened space structures.

Acknowledgments

The research presented herein was supported in part by the Air Force Flight Dynamics Laboratory and the NASA Langley Research Center. The authors appreciate the continued encouragement of Donald B. Paul of the Air Force Flight Dynamics Laboratory and L. Bernard Garrett of NASA Langley Research Center.

References

[1]Sullivan, M.R., "LSST (Hoop/Column) Maypole Antenna Development Program," NASA CR-3558, Parts 1 and 2, June 1982.

[2]Belvin, W.K., "Vibration and Buckling Studies of Pretensioned Structures," Third Annual Technical Review on Large Space Systems Technology, NASA CP-2215, Part 1, Nov. 1981, pp. 109-121. 1981, NASA CP-2215, Part 1, pp. 109-121.

[3]Coyner, J.V., Herbert, J.J., and Bachtell, E. E., "15-Meter Diameter Mechanically Scanned Deployable Antenna," NASA CR-170576, April 1982.

[4]Huebner, K. and Thornton, E.A., "The Finite Element Method for Engineers, 2nd Ed., John Wiley, New York, 1982.

[5]Stricklin, J.A., Haisler, W.E., and Riesemann, W.A., "Geometrically Nonlinear Structural Analysis by Direct Stiffness Method," *Journal of Structural Division, Proceedings of ASCE,* Vol. 97, Sept. 1971, pp. 2299-2314.

[6]Thornton, E.A., Dechaumphai, P., and Pandey, A.K., "Finite Element Thermal-Structural Analysis of Cable-Stiffened Space Structures," Final Report for NASA Research Grant NAG-1-257, submitted April 1984.